Received: 9 November 2022 | Revised: 6 March 2023 | Accepted: 7 March 2023

DOI: 10.1002/est2.464

RESEARCH ARTICLE

ENERGY STORAGE WILEY

Optimal sizing of RES and BESS in networked microgrids based on proportional peer-to-peer and peer-to-grid energy trading

Vankudoth Lokesh | **Altaf Q. H. Badar**

Department of Electrical Engineering, National Institute of Technology Warangal, Warangal 506004, India

Correspondence
Vankudoth Lokesh, Department of Electrical Engineering, National Institute of Technology Warangal, Warangal 506004, India.
Email: vlokesh@student.nitw.ac.in

Abstract

Networked microgrids emerged from the growing deployment of microgrids in the distribution network. The coordinated operation of networked microgrids offers technical and economical benefits to microgrid owners, customers, grid/utility, and other stakeholders. The optimal capacity sizing of renewable energy sources and battery energy storage systems allows microgrids to minimize costs and maximize reliability. A multi-objective optimization problem is developed for optimal sizing in a networked microgrid consisting of four different microgrids. The annual energy costs and loss of power supply probability index are taken as objectives. Peer-to-peer and peer-to-grid energy trading approaches are employed. The peer-to-peer energy trading among microgrids employs the proposed "proportional trading method" via a networked microgrid manager or aggregator. The multi-objective optimization problem formulated is solved using Multi-Objective Particle Swarm Optimization. The individual objective optimization results for annual energy cost and loss of power supply probability are also analyzed. The proposed method decreases the interaction between the grid and the MGs, and the usage of renewable energy sources is enhanced. The capacity of battery energy storage systems is lowered by 96%, 53.2%, 48.86%, 21% for respective microgrids in networked microgrids. The results of proportional peer-to-peer energy trading-based multi-objective optimization show that trading energy among microgrids minimizes annual energy cost by 0.75% while maintaining system reliability.

KEYWORDS

battery energy storage system, multi-objective optimization, multi-objective particle swarm optimization, networked microgrids, peer-to-peer energy trading, peer-to-grid energy trading, photo-voltaic, wind turbine

1 | INTRODUCTION

INCREASING deployment of the DGs into the electrical grid is observed to address the issues such as energy source limitations, carbon emissions, aging infrastructure, rising energy consumption, and energy security concerns. With DGs, sustainable energy is becoming increasingly viable worldwide because they rely significantly on RES (primarily solar PV and WT). However, the stochastic nature of solar PV, WT, etc., and inelastic loads result in a supply-load mismatch. These imbalances can be addressed by ESS. Furthermore, using DG in conjunction with ESS moves the energy paradigm toward decentralization. The weighted Levelized Cost of Electricity (LCOE) of solar PV and onshore wind energy fell 88% and 68%, respectively, from 2010 to 2021.[1] The LCOS of BESS is expected to be reduced by one-third by 2030 and a half by 2050,[2] and the energy capacity to weighted-average installed costs decreased by 72% between 2015 and 2019.[3]

The notion of MGs is developed to maximize on the benefits of DERs (DGs and ESS).[4] In terms of grid characteristics, MG is considered self-sufficient, with DGs, ESS, and controlled loads working as a single entity inside a specific electrical boundary.[5] The MG supports two modes of operation: grid-connected and islanded. In grid-connected mode, the MG can connect to the grid, trade energy, and provide ancillary services. In islanded mode, the MG is disconnected from the grid and is exclusively responsible for the system's reliability, power quality, and security. MGs are positioned near the consumption sites at low or medium-voltage levels. MGs offer a high potential for electrical system enhancement by handling variability, enhancing power quality and reliability, enabling local self-healing, minimizing investment costs, cutting carbon emissions, and decreasing distribution network power losses.[6]

To maximize the benefits for MGs, adequate sizing of DERs is required because of varied characteristics of generating resources. The optimal size minimizes operating costs by assuring minimal investment, optimal DER utilization, and operation at optimal conditions in response to load demands.[7] In literature, the optimal sizing in individual MGs is performed considering various objectives and different techniques. In Reference 8, optimization problem with three objectives, that is, cost, DPSP and REDR, is solved using improved multi-objective grey wolf optimization for an isolated MG. In Reference 9, for sizing an autonomous hybrid MG of a village, a multi-objective problem considering LCOE, LPSP, and REF is solved using multi-modal delayed PSO algorithm.

Similarly, the optimal sizing is performed for an integrated MG considering COE and LPSP using social spider optimizer for Alijouf region.[10] In Reference 11, the autonomous hybrid MG design is assessed by determining the dynamic energy pricing and evaluating the steady-state and transient behavior of the system. The multi-objective problem considering TNPC, COE, and uncertainty in RES is solved using MOPSO. In Reference 12, optimal sizing of an industrial MG is performed considering the effect of DR. The objectives of the problem are to minimize the LCC and CO_2 emissions which is solved using genetic algorithm. Similarly, the optimal sizing of real-world MGs is studied in References 13,14.

Recently, with growth in the number of MGs with diverse features, the MMGs or NMGs framework is proposed in the literature. In the distribution network of a regional power system, these interconnected MGs forming NMGs are geographically near to each other. Different MGs have varying generation and load curves during the day. At any given time, the quantity of energy generated by local RES in the MGs may be higher or lower than the local demand in MGs. In the event of a power deficit, MGs obtain power from the utility grid, which may be costly. The NMG architecture allows the interconnected MGs to trade energy with the connected MGs. Energy trading among MGs enables the NMGs to optimize their economic benefits, maximize the use of DERs, reduce losses, and maximize security and reliability.[15] The primary issue in energy trading is the extent of participation of an individual MG in the total energy traded within the NMG framework. For this, we propose a proportional-based P2P energy trading among the MGs, to be considered while determining optimal sizes of RES and BESS.

In Reference 16, the ideal size for NMGs is determined by taking resilience and cost into account using a three-level approach. The proposed approach incorporates the adaptive genetic algorithm, the non-dominated sorting genetic algorithm-II, and the time-coupled AC-optimal power flow. To increase the resilience and reliability, in Reference 17, optimal sizing of the ESS is studied for NMG. This problem is modeled as a bi-level problem, reduced to a single-level problem, and solved using mixed-integer linear programming. Boundaries, optimum size, and siting of DGs for various MGs are proposed in Reference 18. The imperialist competitive algorithm is used to optimize the operating costs of MMG by determining DG placement and size in regard to load allocation. After the DGs are assigned, the borders of the MGs are determined based on all geographical and electrical constraints, but power trade between MMGs is not considered. The optimal siting, sizing, type, and dispatch of DERs, including allocation of section switches, are proposed in Reference 19. The objective is modeled as mixed-integer linear programming and solved using MOPSO. In Reference 20, the appropriate placement and size of various components in various buildings acting as smart MGs for a pilot project in Iran are discussed. Sizing and siting are done to lower MG costs and losses, respectively, using PSO. This study does not address the topic of trading amongst MGs. In Reference 21, a two-stage NMG planning strategy is given, with the first stage centered on minimizing MG's yearly investment costs. While the second stage focuses on reducing daily operating expenses in both grid-connected and island modes. In Reference 22, a case study in Adelaide is provided to minimize the total yearly cost to fulfill the annual load demand. According to this study, an individual home in the area acts as an MG, and together these homes form an MMG framework. The study shows that MMG decreases DG capacity needed for installation and enhances grid interaction.

RE generation planning is studied in Reference 23, considering the long-term investment and short-term operating costs. A Nash bargaining mechanism is used to divide the costs among the MGs. The energy exchange between MG and grid is not taken into account in this study. Optimal sizing of DG, ES, and the market clearing price for energy trading is accomplished in Reference 24. Interaction between the MMG and real-time electricity market is considered to reduce the MMG's overall cost. The Cournot equilibrium determines the market-clearing price, while optimal decision variables are determined using quantum-PSO. To reduce operational expenses,[25] considers optimum planning of single and multi-carrier MGs. The problem addresses all the technical, environmental, and mechanical limitations while obtaining the optimal sizing according to the change in load for every season. The optimal capacity allocation of RES and BESS is determined to maximize the AEP in Reference 26. The problem is considered as a cooperative game and solved for nash bargaining solution using PSO. In References 27,28, nash equilibrium and cooperative game are proposed, respectively, for multi-objective game theoretic problem in RES and BESS capacity allocation. PSO is applied in both works with the objective to maximize AEP and reliability.

The literature studied does not consider the trading of energy through NMG manager/aggregator among sellers and buyers for determining ideal sizes of RES and BESS. In the proposed research work, we focus on designing the optimal capacity sizing of RES and BESS of each MG in an NMG framework considering a proportional method for trading energy among sellers and buyers. The contributions of the paper can be listed as:

1. The optimal sizing of RES and BESS is performed for MGs in the NMG framework through a multi-objective problem of minimizing AEC and maximizing reliability.
2. The proportional energy trading approach is proposed for P2P energy trading between buyers and sellers.
3. Individual objectives are optimized separately using PSO and compared with the optimal results obtained through the multi-objective problem using MOPSO, considering P2G trading and P2P trading individually.

This article is categorized into five sections: Section 2 discusses the NMG framework, the modeling of components of each MG for the NMG framework, and the proportional P2P trading approach. Subsequently, Section 3 gives the problem formulation for minimizing AEC and LPSP. Section 4 presents the solution methodology for solving the problem, that is, using PSO and MOPSO methodologies. Section 5 describes the data considered for the study and the results obtained. Finally, in Section 6, the conclusions are presented.

2 | NMG MODEL AND ENERGY TRADING FORMULATION

The NMG topology considered in this study is described, and modeling of various components such as PV, WT, BESS, and loads of each MG in the NMG framework is discussed in this section. Also, the proportional P2P energy trading scheme is formulated.

2.1 | NMG topology

This paper aims to determine the optimal capacity of PV-WT-BESS in an NMG considering proportional P2P trading. For this, we implement a modified version of the standard NMG benchmark system described in Reference 29. In the system, each MG is connected to the grid at different locations and interconnected with other MGs via tie-lines. This allows energy trading among MGs and the grid directly through the NMG manager or aggregator and DNO. The schematic of NMGs' trading strategy is depicted in Figure 1. Each MG is considered to consist of PV or WT or both of them along with loads and BESS. Each MG in the system has an MGO responsible for managing energy in the corresponding MG. NMG manager or aggregator receives the deficit/excess energy information from the MGs and the energy is dispatched among peer MGs based on a proportional approach. Here we consider the DNO, which acts as an operator for P2G trading. It decides the electricity selling and buying prices with the grid. For P2P trading amongst MGs the prices for energy trading in the NMG framework are determined by the NMG manager or aggregator.

2.2 | NMG modeling

This section discusses the modeling of PV, WT, load, and BESS for each MG in the NMG framework.

2.2.1 | PV, wind, and load modeling

The hour-wise PV and WT generation, along with the load data are statistically modeled according to Reference 29 as mentioned in Equations (1)-(3). The constraints for

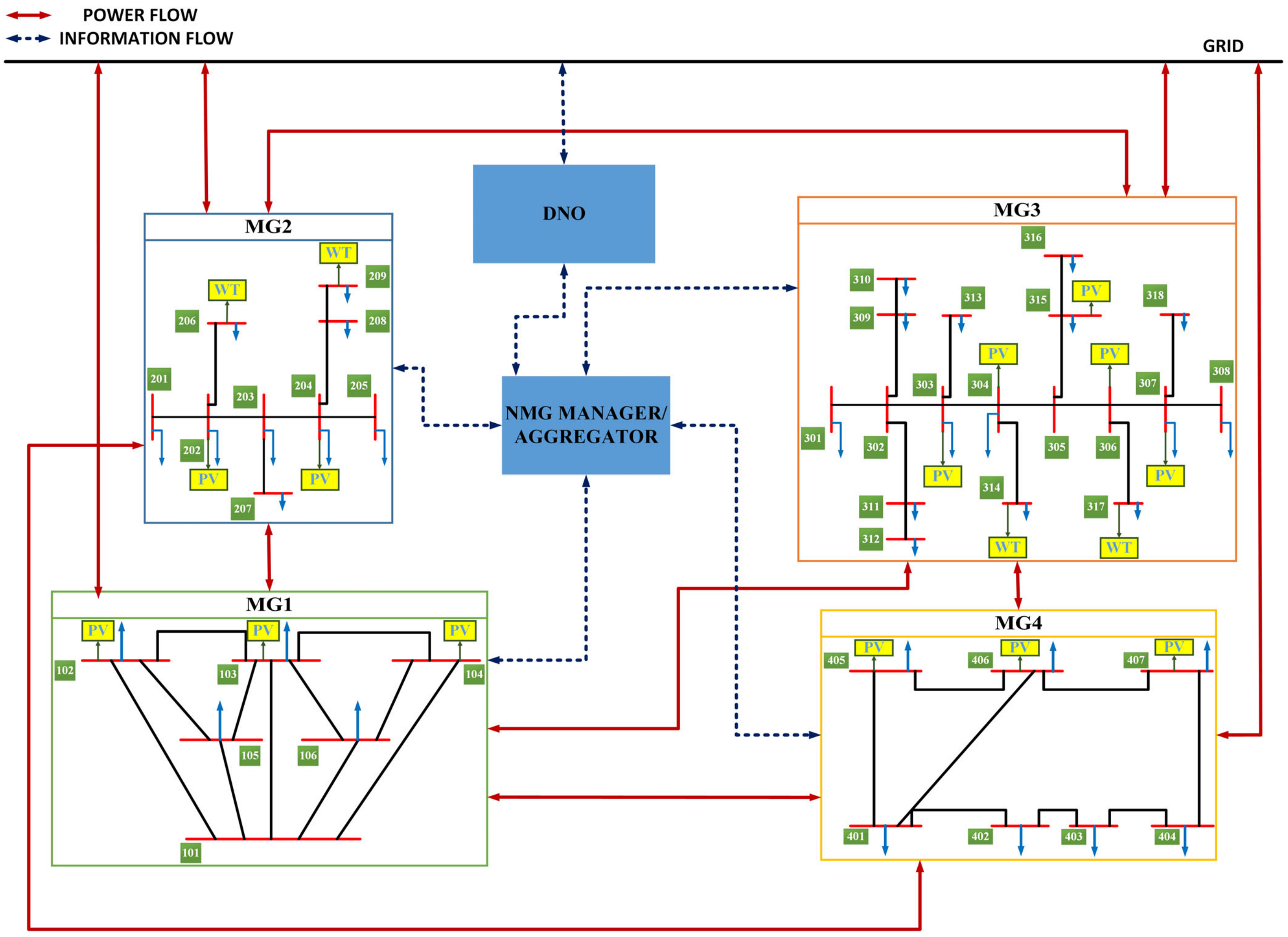

FIGURE 1 Modified single line diagram of NMG.[29]

maximum WT and PV capacity for generation are given in Equations (4) and (5).

$$ld_i^t = \frac{\%ld_i^{w,t}}{100} * \frac{\%ld_i^{d,t}}{100} * ld_{cy,i} \quad \forall i \in \{1,N\} \tag{1}$$

$$PV_i^t = \frac{\%PV_{al,i}^t}{100} * PV_{cy,i} \quad \forall i \in \{1,N\} \tag{2}$$

$$W_i^t = \frac{\%W_{al,i}^t}{100} * W_{cy,i} \quad \forall i \in \{1,N\} \tag{3}$$

$$PV_{\min,i} \le PV_i^t \le PV_{\max,i} \quad \forall i \in \{1,N\} \tag{4}$$

$$W_{\min,i} \le W_i^t \le W_{\max,i} \quad \forall i \in \{1,N\} \tag{5}$$

2.2.2 | Battery energy storage system modeling

The BESS allows the storage of electrical energy for use at a later time. This improves the flexibility and adaptability of the system. BESS is characterized by the charging and discharging of power. The BESS is charged by the MG whenever the RE generation is greater than the load $(PV_i^t + W_i^t > ld_i^t)$ and when $BE_i^t < BE_i^{\max}$. Similarly, it discharges whenever the RE generation is lesser than the load in an MG $(PV_i^t + W_i^t < ld_i^t)$ and when $BE_i^t > BE_i^{\min}$. The maximum charging and discharging power constraints for BESS at a particular time are given by Equations (6) and (7). The energy capacity of BESS at a specific hour is given by Equation (8). The energy stored in the BESS is limited by Equation (9). The flowchart of BESS scheduling is given in Figure 2.

$$BP_{i,c}^{\min} \le BP_{i,c}^t \le BP_{i,c}^{\max} \quad \forall i \in \{1,N\} \tag{6}$$

$$BP_{i,d}^{\min} \le BP_{i,d}^t \le BP_{i,d}^{\max} \quad \forall i \in \{1,N\} \tag{7}$$

$$BE_i^t = BE_i^{t-1} + \left(BP_{i,c}^t * \eta_c * \Delta(h) - \frac{BP_{i,d}^t}{\eta_d} * \Delta(h) \right) \quad \forall i \in \{1,N\} \tag{8}$$

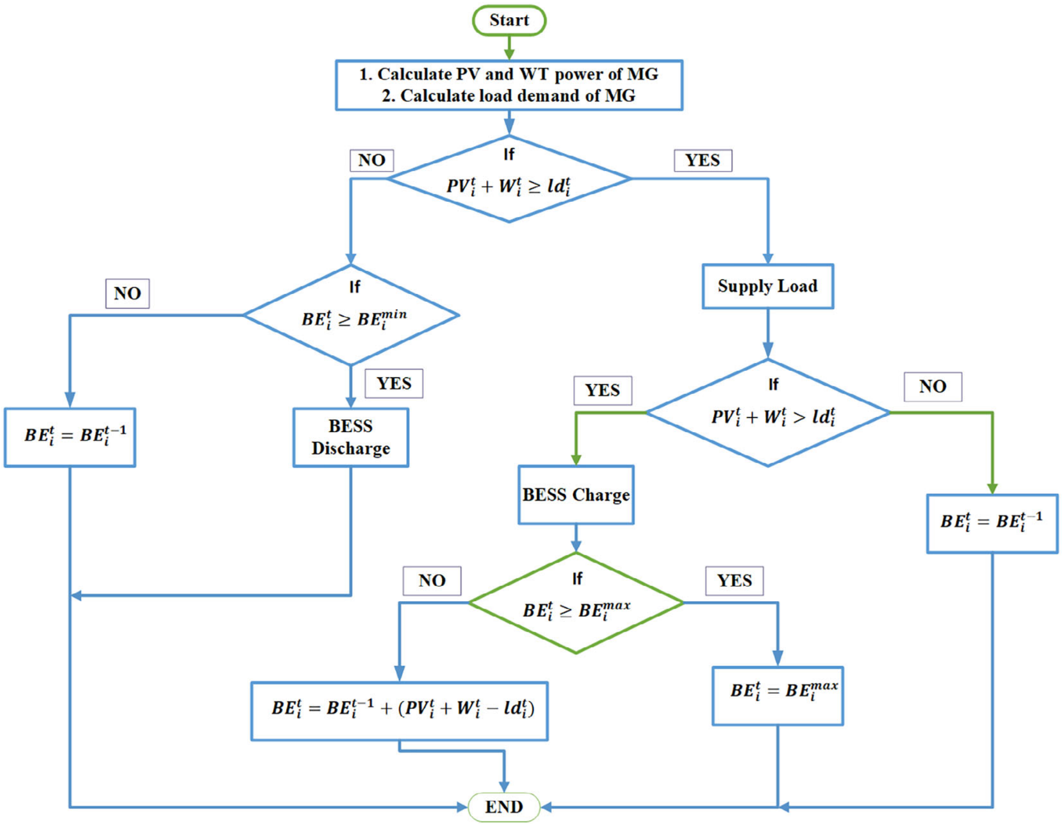

FIGURE 2 BESS scheduling in MG.

$$BE_i^{\min} \le BE_i^t \le BE_i^{\max} \quad \forall i \in \{1, N\} \tag{9}$$

where η_c and η_d are considered as 0.95 and 0.92.[29] $\Delta(h)$ is the time period for which the battery is charging or discharging that is, 1 hour.

2.3 | Energy Trading Strategy in NMG

Energy is either excess or deficit in an MG at a given hour (t), depending on the load and generation balance in the corresponding MG. If $PV_i^t + W_i^t > ld_i^t$ where $i \in \{1, N\}$, at a particular hour, then the MG_i, initially stores excess energy in the BESS, as per the strategy. If the MG still has excess energy remaining after charging BESS, then MG_i acts as a seller in the NMG framework. In a contrary case, where $PV_i^t + W_i^t < ld_i^t$, MG_i will discharge BESS to meet the load demand. If the load is still not satisfied, MG_i is required to buy energy and acts as a buyer. S represents the set of all MGs with excess energy, whereas B is the set of MGs with deficit energy. Equation (10) gives the excess/deficit energy in MG_i at time "t" based on the set it belongs to, that is, either set S or B.

$$MG_{i,sur}^t = \begin{cases} \left(PV_i^t + W_i^t - \left(BE_i^{t-1} + BP_{i,c}^t * \eta_c * \Delta(h)\right) - ld_i^t\right) & \forall i \in S \\ \left(PV_i^t + W_i^t + \left(BE_i^{t-1} - \dfrac{BP_{i,d}^t}{\eta_d} * \Delta(h)\right) - ld_i^t\right) & \forall i \in B \end{cases} \tag{10}$$

The total amount of excess/deficit energy with seller MGs and buyer MGs is given in Equations (11) and (12) respectively.

$$E_{T,ex}^t = \sum_{i=1}^{S} \left(MG_{i,sur}^t\right) \quad \forall \;\; S \subset N \tag{11}$$

$$E_{T,df}^t = \sum_{i=1}^{B} \left(MG_{i,sur}^t\right) \quad \forall \;\; B \subset N \tag{12}$$

Excess energy from the seller MG is sold according to the proportional sharing method as given in Equation (13) and the amount of energy received by the buyer MG, is given by Equation (14), for different conditions.

$$PMG_{s,i}^t = \begin{cases} \dfrac{MG_{i,sur}^t}{E_{T,df}^t * E_{T,ex}^t} & \text{if } \left(E_{T,df}^t + E_{T,ex}^t \ge 0\right) \\ MG_{i,sur}^t & \text{if } \left(E_{T,df}^t + E_{T,ex}^t < 0\right) \end{cases} \tag{13}$$

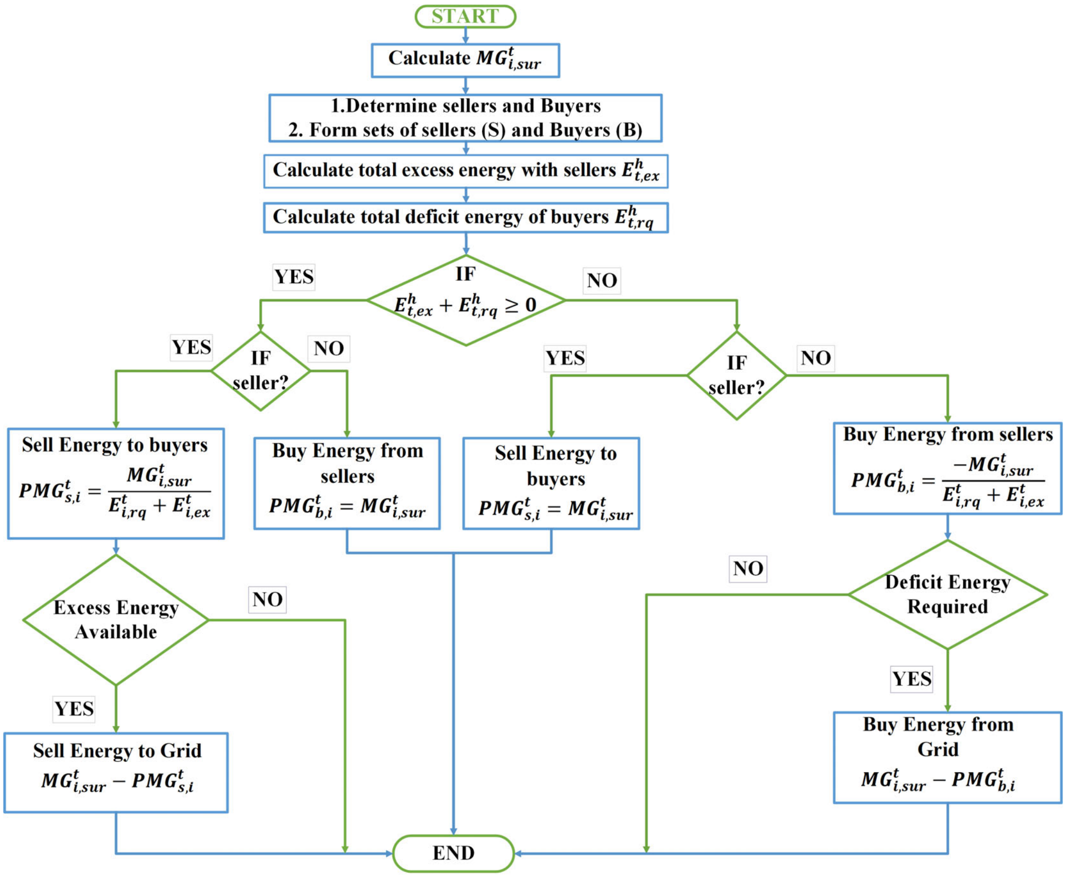

FIGURE 3 Proportional P2P energy trading in NMG.

$$PMG^t_{b,i} = \begin{cases} MG^t_{i,sur} & \text{if } \left(E^t_{T,df} + E^t_{T,ex} \geq 0\right) \\ \dfrac{-MG^t_{i,sur}}{E^t_{T,df} * E^t_{T,ex}} & \text{if } \left(E^t_{T,df} + E^t_{T,ex} < 0\right) \end{cases} \tag{14}$$

The excess energy remaining with seller MGs after trading among the NMGs is sold to the grid, and vice versa for buyer MGs, as given in Equation (15). The flowchart for energy trading in the NMGs based on proportional sharing is shown in Figure 3. The total energy generated, energy traded within MGs and the grid must satisfy the total load in the NMG framework.

$$PG^t_{s,b,i} = \begin{cases} MG^t_{i,sur} - PMG^t_{s,i} & \text{if } \left(MG^t_{i,sur} \geq 0\right) \\ MG^t_{i,sur} - PMG^t_{b,i} & \text{if } \left(MG^t_{i,sur} < 0\right) \end{cases} \tag{15}$$

3 | PROBLEM FORMULATION

The objective of this study is to optimize the capacity of PV-WT-BESS in the NMG system considering P2P energy such that minimum AEC is achieved while guaranteeing reliable power. The reliability of power is calculated using the index LPSP.

3.1 | Annual energy cost

AEC depends on several parameters: income from power utilization of RES and BESS, salvage income, investment cost, operation, and maintenance cost, the cost of energy traded with the grid, and NMG framework. The AEC for each MG is given by Equation (16). The AEC for the total NMG framework is given by Equation (17).

$$AEC_i = C_i^{INV} + C_i^{O\&M} - I_i^{U,RE} - I_i^{U,B} - I_i^{SL} - C_i^{EC} \tag{16}$$

$$AEC_{NMG} = \sum_i^N AEC_i \quad \forall i \in \{1,N\} \tag{17}$$

3.1.1 | Investment cost

The amortized cost for installing the RES and BESS is determined using Equation (18).

$$C_i^{INV} = P_i^{G,cy} * E_i^{IC} * \frac{D(1+D)^{L_i}}{\left((1+D)^{L_i}-1\right)} \tag{18}$$

3.1.2 | Operation and maintenance cost (O&M)

The O&M cost of RES and BESS is obtained using Equation (19).

$$C_i^{O\&M} = P_i^{G,cy} * E_i^{O\&M} \tag{19}$$

3.1.3 | Income from utilization of RE generation

The total RE power generated during "t" is given in Equation (20). The amount of RE utilized in an MG during each "t" depends on the total RE power generated and load as given by Equation (21). The income generated for energy utilized from RES in each MG is given in Equation (22).

$$P_i^{G,RE,t} = PV_i^t + W_i^t \tag{20}$$

$$P_i^{U,RE,t} = \begin{cases} PV_i^t + W_i^t & P_i^{G,RE,t} \le ld_i^t \\ ld_i^t & P_i^{G,RE,t} > ld_i^t \end{cases} \tag{21}$$

$$I_i^{U,RE} = \sum_{t=1}^{T} E_{p,b}^t * P_i^{U,RE,t} \tag{22}$$

3.1.4 | Income from utilization of BESS

The battery is discharged whenever the load exceeds the total RES power generated and vice versa, based on different constraints. The total power consumed in MG is given in Equation (23). Annual income generated from the utilization of BESS is given in Equation (24).

$$P_{i,CD}^t = ld_i^t + \left(BE_i^t - BE_i^{t-1}\right) \tag{23}$$

$$I_i^{U,B} = \sum_{t=1}^{T} E_{p,b}^t * \left(BE_i^t - BE_i^{t-1}\right) \tag{24}$$

3.1.5 | Salvage income

This is the income generated by selling the RES and BESS equipment at the end of their useful life. The salvage income from BESS is neglected. The salvage income values for RES are calculated using Equation (25).

$$I_i^{SI} = P_i^{G,cy} * E_i^{SI} * \frac{D}{\left((1+D)^{L_i}-1\right)} \tag{25}$$

3.1.6 | Cost of energy traded with grid and NMG

The cost of energy traded with the main grid is given in Equation (26). The cost for energy traded within the NMG framework is given using Equation (27). The total cost of energy traded is given in Equation (28). The costs would be negative when energy is sold by the MG and vice versa.

$$C_i^{EG,t} = PG_{s,b,i}^t * E_{p,s,b}^t \tag{26}$$

$$C_i^{EMG,t} = PMG_{b,s,i}^t * E_{p,MG}^t \tag{27}$$

$$C_i^{EC} = \sum_{i=1}^{T} \left(C_i^{EG,t} + C_i^{EMG,t}\right) \tag{28}$$

3.2 | Loss of power supply probability

The reliability of the NMG is calculated using the index of LPSP. The LPSP is used to measure the probability that optimized PV, WT, and BESS capacity, can satisfy the load demand in the corresponding MG. The LPSP is calculated as the total number of hours the load is not satisfied divided by the total evaluation period. The value of LPSP is in the range [0,1]. If the power generated from the optimized RES and BESS satisfies the demand at each hour, LPSP converges to zero. For a single MG, the LPSP is calculated using Equation (29).

$$LPSP_{MG_i} = \frac{\sum_{t=1}^{T} H_t}{T} \tag{29}$$

$$H_t = \begin{cases} 1 & \text{if} \left(ld_i^t - PV_i^t - W_i^t + \left(\frac{BE_i^t - BE_i^{t-1}}{\Delta(h)} \right) \right) > 0 \\ 0 & \text{otherwise} \end{cases} \tag{30}$$

where H_t returns 1 when the optimized hybrid RESs and battery do not satisfy the load for the tth hour and 0 for all other cases.

For the NMG, LPSP and its calculation considering the P2P energy trading is given in Equation (31). In the

NMG framework, the additional power with the seller MG is sold to the buyer MGs in proportion and the remaining excess/deficit energy after selling/buying is sold/bought from the main grid.

$$LPSP_{NMG} = \left(\frac{\sum_{i=1}^{N} LPSP_{MG_i}}{N} \right) \forall \ i \in 1,2,\ldots,N \tag{31}$$

The multiple objectives of the problem under consideration, are to minimize the AEC and simultaneously minimize LPSP as given by Equation (32).

$$F = \min[AEC_{NMG}, LPSP_{NMG}] \tag{32}$$

In summary, the objective of the problem is to obtain optimal capacity of RESs and BESS to minimize the AEC and simultaneously minimize LPSP while considering P2P energy trading among the MGs. In P2P trading the energy is traded in a proportional manner among buyers and sellers.

4 | MULTI-OBJECTIVE OPTIMIZATION (MOO)

MOO is used for solving problems with multiple objective functions which can be either conflicting or agreeing.

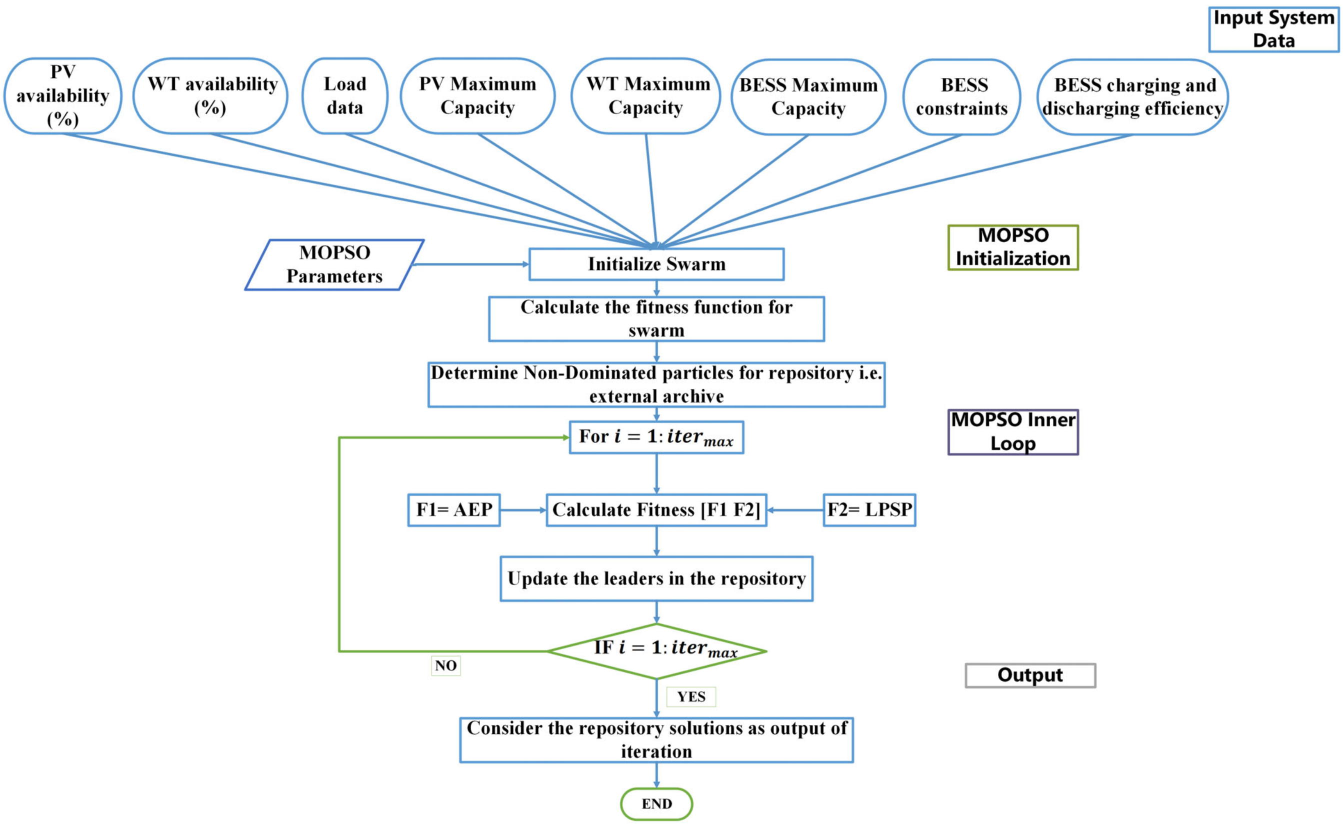

FIGURE 4 Flowchart for the implementation of MOPSO for minimization AEC and LPSP.

TABLE 1 Details of MGs in NMG system.[29]

MGs	Buses	Lines	PV range (kW)		WT range (kW)		BESS range			
							Energy (kWh)		Power (kW)	
			Min	Max	Min	Max	Min	Max	Min	Max
MG1	6	11	0	6400	0	0	0	10 000	0	6400
MG2	9	8	0	5600	0	1300	0	12 000	0	5600
MG3	18	17	0	5600	0	1700	0	12 400	0	5600
MG4	7	8	0	5600	0	0	0	12 000	0	5600

The MOO either minimizes or maximizes multiple conflicting objective functions, as described in Equation (33).

$$\begin{aligned} &\text{Minimize} \quad F(x) = [f_1(x), f_2(x), \ldots, f_n(x)] \\ &\text{subject to} \\ &g_i(x) \le 0, \quad i = 1, 2, \ldots, m \\ &h_i(x) = 0, \quad i = 1, 2, \ldots, k \end{aligned} \tag{33}$$

where x is the decision variable vector, $f_i(x)$.

$i = 1, \ldots, n$ are the objective functions of x to be minimized or maximized, and $g_i(x)$ and $h_i(x)$ are the constraint functions for the problem. The MOPSO approach is considered in this paper to solve the considered multi-objective problem.

4.1 | Particle Swarm Optimization (PSO)

PSO is a heuristic technique based on the social behavior of birds inside a flock.[30] This is a simplistic population-based approach. Each particle in PSO defines a feasible solution to the defined problem. The particles in PSO, travel through the hyper-dimensional search space and changes their position within the search space to probe optimal result. Each particle in PSO is associated with the particle's best position and global best position. These particle's path relies on the particle's velocity set in a certain direction depending on the particle's personal best and global best that is, the particle's personal flying experience and its neighbors.[31]

4.1.1 | PSO for single objective functions

In single objective optimization, the position of particles is changed based on the particle's personal flying experience and neighborhood experience, as in Equation (34).

$$x_i^t = x_i^{t-1} + v_i^t \tag{34}$$

where x_i^t is the position of the particle p_i at time "t." The velocity v_i^t is added to this position. The velocity is defined as given in Equation (35).

$$\begin{aligned} v_i^t = \omega * v_i^{t-1} + c_1 * rand() * \left(x_{pbest_i} - x_i^t\right) \\ + c_2 * Rand() * \left(x_{gbest_i} - x_i^t\right) \end{aligned} \tag{35}$$

where ω is the inertia constant, rand() and Rand() are random values $\in [0,1]$. x_{pbest_i} and x_{gbest_i} are the personal best and global best of the particle "i." c_1 and c_2 are the acceleration coefficients.

4.1.2 | MOPSO

In comparison to PSO, in MOPSO, each objective function has its own neighborhood to update its position.[32] The velocity update of particles for MOPSO is given in Equation (36). The global best particle for each objective function is stored in the repository. The values stored in the repository (REP) are non-dominated results and are used for updating the particles. The mutation operator is applied to increase the diversity of the search in order to obtain the optimal solution.[33] The particles stored in the repository after convergence are considered solutions. The step-by-step procedure for MOPSO is presented in Algorithm 1.

$$\begin{aligned} v_i^t = \omega * v_i^{t-1} + c_1 * rand() * \left(x_{pbest_i} - x_i^t\right) \\ + c_2 * Rand() * \left(REP(h) - x_i^t\right) \end{aligned} \tag{36}$$

where $REP(h)$ is a value considered from the repository.

ALGORITHM 1 Algorithm for MOPSO

Require: $c_1, c_2, w, iter_{\max}, swarmsize, repositorysize$
Require: $gridsize, mutationrate, InflationRate$
Require: $LeaderSelectionPressure$, $DeletionSelectionPressure$
 Initialize Swarm.
 Initialize leaders into the repository that is, external archive.
 for $i = 1 : iter_{\max}$ **do**
  Select Leader
  for $i = 1 : swarmsize$ **do**
   Update Velocity using Equation (36).
   Update Particle Position using Equation (34).
   Verify if the particles are satisfying constraints.
   Calculate Fitness.
   Apply Mutation.
   Calculate Fitness.
   Check for Dominance.
   Update Personal Best.
  end for
  Update leaders in the repository.
  $i = i{+}{+}$
  if $i = iter_{\max}$ **then**
   Get Results from the external archive.
  end if
 end for

The step-by-step procedure for minimization of AEC and LPSP problem as MOO using MOPSO is shown in Figure 4.

5 | RESULTS AND DISCUSSIONS

NMG system given in Reference 29 is modified in this paper as shown in Figure 1, for the implementation of the proposed method. The modified system is considered to be interconnected among each other for trading and the conventional generation is neglected from the standard benchmark system. The system consists of four distinct MGs ($N = 4$), where first bus of each MG is considered as a slack bus. The maximum capacity of PV, WT, and BESS permitted in each MG and details of NMG are shown in Table 1. The input parameters considered for calculations are shown in Table 2.[27] The optimization is applied for annual data but for representation purposes we have shown results for single day. The optimization techniques are implemented in MATLAB software.

The results in this study are presented in a 2-fold manner. First, we analyze the AEC and LPSP individually using PSO for both the P2G trading and P2P trading scheme. Then an analysis for the same NMG framework considering multi-objective optimization using MOPSO for both trading schemes is presented. The prices for trading are assumed to be fixed and given in Table 3.

TABLE 2 Input parameters for NMG.[27]

Parameters	Value
D	12%
L_{WT}	20 years
E_{WT}^{IC}	770 $/kW
$E_{WT}^{O\&M}$	20 $/(kW.year)
E_{PV}^{IC}	1890 $/kW
L_{PV}	20 years
$E_{PV}^{O\&M}$	20 $/(kW.year)
L_{BESS}	10 years
E_{BESS}^{IC}	100 $/kW
$E_{BESS}^{O\&M}$	1 $/(kW.year)
E_{WT}^{si}	77 $/kW
E_{PV}^{si}	189 $/kW

TABLE 3 Energy trading prices.[27]

Parameters	Value
($E_{p,MG}^{t}$)	0.15 $/kWh
($E_{p,s}^{t}$)	0.10 $/kWh
($E_{p,b}^{t}$)	0.28 $/kWh

5.1 | Optimization of individual objectives using PSO

In this section, the results for the minimization of AEC and LPSP as individual objectives, using PSO are presented. The optimum RES and BESS sizes for each objective are compared in Tables 4 and 5. The PSO is run for 200 iterations, 100 particles, and the acceleration coefficients c_1 and c_2 are considered to be 2. The ω and ω_{damp} are considered to be 1 and 0.99, respectively.

5.1.1 | AEC

For AEC optimization, the cost is reduced for P2P energy trading compared to P2G energy trading as shown in Table 4. The optimal size of BESS for MG_1 and MG_3 obtained is 0 kW. Based on the sizing obtained, the RES generation, the BESS charging and discharging pattern for MGs, amount of energy traded with the grid (PMGG), and among the MGs for P2P energy trading (PMGM) is shown in Figure 5. Similarly for P2G energy trading results are shown in Figure 6.

5.1.2 | LPSP

LPSP is minimized considering P2P energy trading compared to P2G energy trading as shown in Table 5.

TABLE 4 Comparison of P2G and P2P energy trading for AEC using PSO.

MG	Optimal size			P2G energy trading		P2P energy trading	
	PV (kW)	WT (kW)	BESS (kWh)	LPSP	AEC ($)	LPSP	AEC ($)
MG1	6400	0	0	0.95557	37 273 107.21	0.95278	37 252 885.65
MG2	5600	1300	0				
MG3	5600	1700	3716.23				
MG4	5600	0	10 603.05				

TABLE 5 Comparison of P2G and P2P energy trading for LPSP using PSO.

MG	Optimal size			P2G energy trading		P2P energy trading	
	PV (kW)	WT (kW)	BESS (kWh)	LPSP	AEC ($)	LPSP	AEC($)
MG1	6400	0	979.913	0.95184	37 368 050.9	0.95062	37 353 669.22
MG2	5600	1300	12 000				
MG3	5600	1700	9920				
MG4	5600	0	10 375.07				

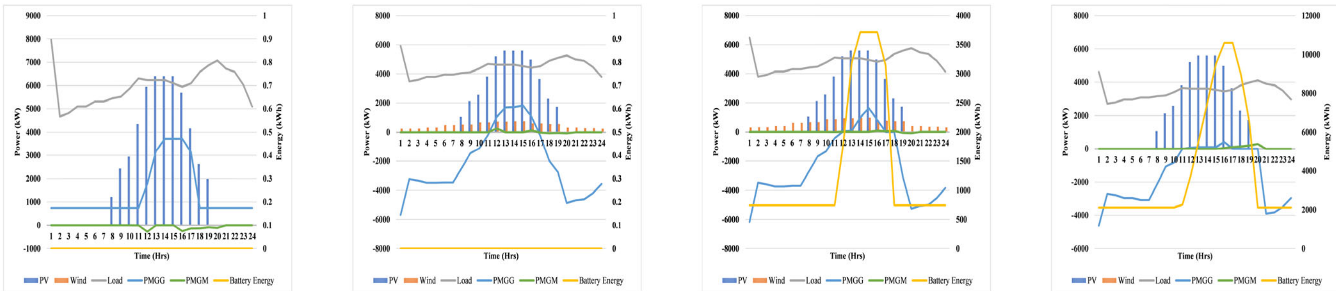

(A) MG1. (B) MG2. (C) MG3. (D) MG4.

FIGURE 5 P2P energy trading pattern for AEC using PSO.

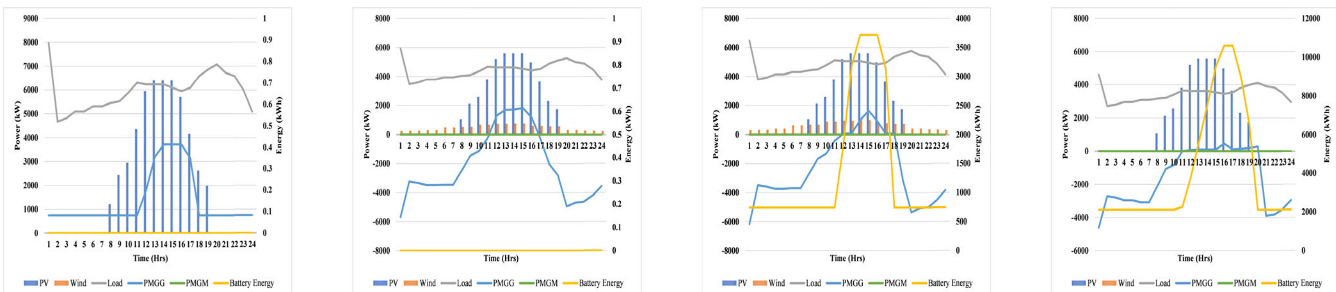

(A) MG1. (B) MG2. (C) MG3. (D) MG4.

FIGURE 6 P2G energy trading pattern for AEC using PSO.

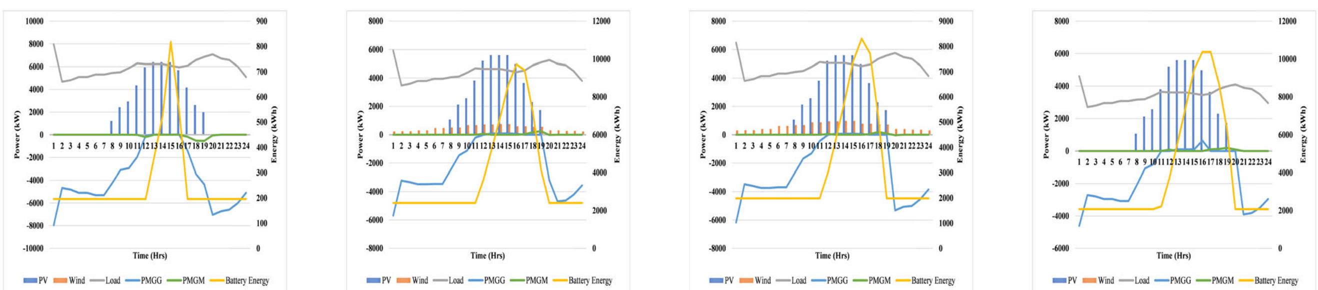

(A) MG1. (B) MG2. (C) MG3. (D) MG4.

FIGURE 7 P2P energy trading pattern for LPSP using PSO.

Considering LPSP, as the objective function, the RES generation, charging and discharging of BESS, energy traded with grid, and among MGs is shown in Figure 7 for P2P energy trading. Similarly, for P2G energy trading, LPSP is minimized, and the results are shown in Figure 8.

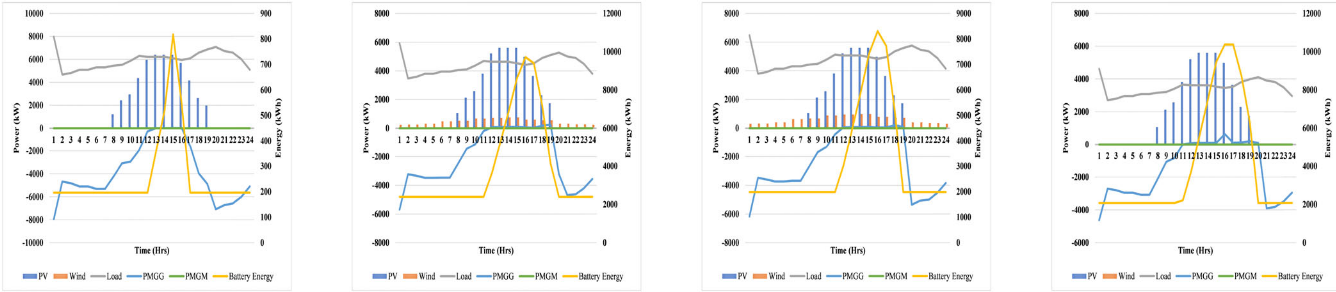

(A) MG1. (B) MG2. (C) MG3. (D) MG4.

FIGURE 8 P2G energy trading pattern for LPSP using PSO.

TABLE 6 Comparison of P2G and P2P energy trading using MOPSO.

MG	Optimal size			P2G energy trading		P2P energy trading	
	PV (kW)	WT (kW)	BESS (kWh)	LPSP	AEC ($)	LPSP	AEC ($)
MG1	6400	0	387.064	0.95278	37 262 735.86	0.95139	37 249 249.21
MG2	5600	1300	5613.047				
MG3	5600	1700	6340.179				
MG4	5600	0	9390.615				

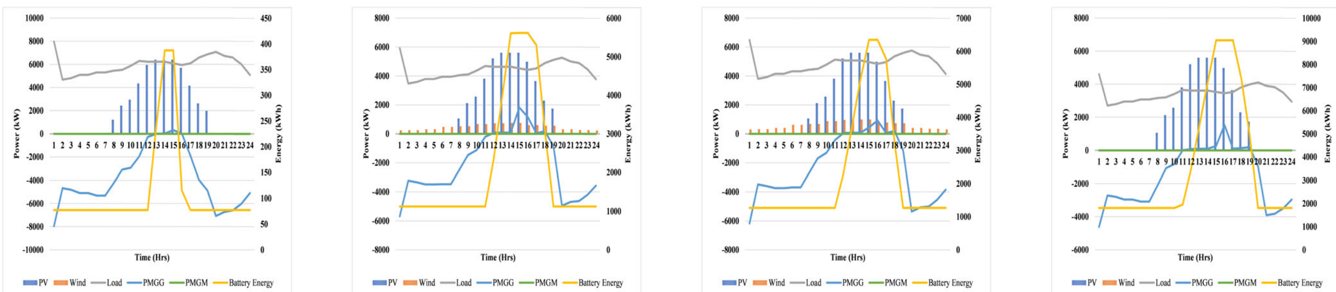

(A) MG1. (B) MG2. (C) MG3. (D) MG4.

FIGURE 9 P2G energy trading pattern using MOPSO.

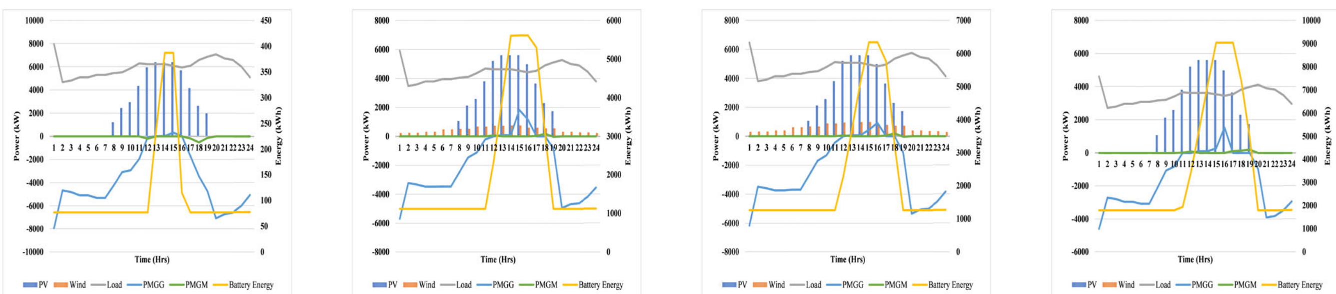

(A) MG1. (B) MG2. (C) MG3. (D) MG4.

FIGURE 10 P2P energy trading pattern using MOPSO.

The optimal size of RES remains the same when AEC and LPSP are optimized individually. The capacity of BESS is more while optimizing the LPSP than AEC. The cost is lower when considering AEC as an objective compared to LPSP. Similarly, while considering LPSP as an objective, reliability is improved as compared to the objective being AEC. In both objectives, the results are better for P2P energy trading when compared with P2G energy trading.

TABLE 7 Comparison of P2P and P2G trading.

Parameter ($)	Maximum capacity	P2G trading	P2P trading
Investment cost MG1	1 753 276.50	1 624 579.69	1 624 579.69
Investment cost MG2	1 711 640.20	1 626 132.45	1 626 132.45
Investment cost MG3	1 758 230.02	1 677 101.87	1 677 101.87
Investment cost MG4	1 577 627.54	1 537 994.27	1 537 994.27
O&M cost MG1	138 000	128 387.06	128 387.06
O&M cost MG2	150 000	143 613.05	143 613.05
O&M cost MG3	158 400	152 340.18	152 340.18
O&M cost MG4	124 000	121 039.61	121 039.61
Cost of trade with grid MG1	−14 369 000.00	−14 388 000.00	−14 370 000.00
Cost of trade with grid MG2	−9 678 900.00	−9 685 900.00	−9 686 500.00
Cost of trade with grid MG3	−10 681 000.00	−10 684 000.00	−10 682 000.00
Cost of trade with grid MG4	−7 517 700.00	−7 519 300.00	−7 524 000.00
Cost of trade with NMG MG1	−9418.60	0.00	−9479.40
Cost of trade with NMG MG2	1822.10	0.00	1988.60
Cost of trade with NMG MG3	260.20	0.00	492.30
Cost of trade with NMG MG4	7336.40	0.00	6998.50
Income utilization of RES MG1	2 856 800.00	2 856 300.00	2 856 300.00
Income utilization of RES MG2	3 126 000.00	3 118 300.00	3 118 300.00
Income utilization of RES MG3	3 333 300.00	3 330 800.00	3 330 800.00
Income utilization of RES MG4	2 438 600.00	2 417 600.00	2 417 600.00
Income utilization of BESS MG1	4183.40	1718.10	1718.10
Income utilization of BESS MG2	64 353.00	52 302.00	52 302.00
Income utilization of BESS MG3	47 288.00	44 914.00	44 914.00
Income utilization of BESS MG4	150 950.00	139 040.00	139 040.00
Salvage income MG1	16 787.77	16 787.77	16 787.77
Salvage income MG2	16 078.57	16 078.57	16 078.57
Salvage income MG3	16 506.03	16 506.03	16 506.03
Salvage income MG4	14 689.30	14 689.30	14 689.30
Annual cost MG1	13 391 675.37	13 266 037.59	13 257 822.07
Annual cost MG2	8 332 292.53	8 268 950.37	8 267 572.08
Annual cost MG3	9 199 735.76	9 120 756.24	9 119 196.24
Annual cost MG4	6 607 773.509	6 606 991.661	6 604 658.82
AEC	37 531 477.18	37 262 735.86	37 249 249.21

TABLE 8 Output for single and multi-objective optimization.

Method	AEC ($)	LPSP
PSO—AEC	37 252 885.65	0.95278
PSO—LPSP	37 353 669.22	0.95062
MOPSO	37 249 249.21	0.95139

5.2 | Multi-objective optimization using MOPSO

In this section, the results for MOO using MOPSO are presented. MOPSO is run for 200 iterations and 100 particles. The MOPSO parameters: repository size is considered to be 100, the acceleration coefficients c_1 and c_2 are considered 2, inflation rate (α) is 0.1, leader selection pressure (β) is 2, deletion selection pressure (γ) is 2, mutation rate (μ) is 0.1, ω is 1 and ω_{damp} is 0.99. The optimum RES and BESS sizes obtained for MOPSO are shown in Table 6. The results for P2G trading and P2P energy trading considering MOPSO are shown in Figures 9 and 10.

From Table 6, the AEC achieved is lesser for P2P trading compared to P2G trading. Also, the LPSP is minimized when considering P2P energy trading. A

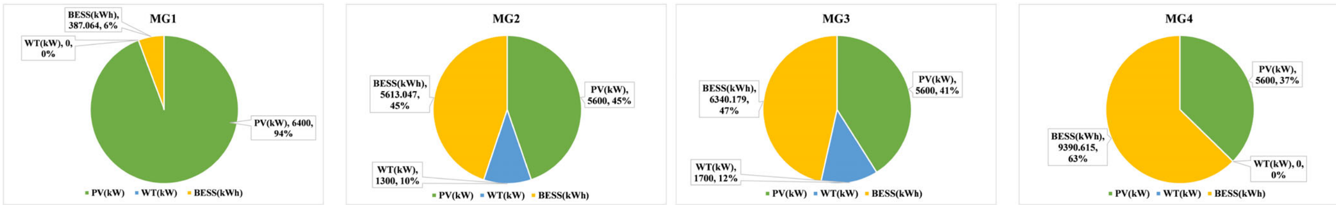

(A) Optimal Capacity of MG_1. (B) Optimal Capacity of MG_2. (C) Optimal Capacity of MG_3. (D) Optimal Capacity of MG_4.

FIGURE 11 Optimal capacity of MGs in NMG.

comparison of various costs and income for different MGs considering P2P and P2G energy trading in the NMG framework using MOPSO is shown in Table 7.

The optimal sizes of RES and BESS in MG_1, MG_2, MG_3 and MG_4 obtained are shown in Figure 11. In Table 8, a comparison of the different single objective results obtained through PSO and multi-objective result obtained through MOPSO is shown.

6 | CONCLUSION

The optimal sizing of RES and BESS for MGs in the NMG framework is presented in this research, with cost minimization and reliability enhancement as objectives. While determining the ideal sizes of RES and BESS for MGs, two energy trading schemes, P2G and P2P, based on a proportional sharing approach, are employed. A MOO problem is modeled and implemented using MOPSO. P2P energy trading among MGs reduces cost and increases reliability when compared to P2G energy trading. The difference in cost between maximum capacity and optimal capacity obtained through P2P energy trading using proportional sharing for each MG is: MG_1—133 853.30 ($), MG_2—64 720.45 ($), MG_3—80 539.52 ($), MG_4—3114.69 ($). As a result, the quantity of RES utilization is maximized, the interaction with the grid is decreased, and the BESS capacity required is lowered through P2P energy trading using a proportional sharing approach.

NOMENCLATURE

Acronyms

AEC	annual energy cost
AEP	annual energy profit
BESS	battery energy storage system
COE	cost of energy
D	discount rate
DER	distributed energy resource
DG	distributed generation
DNO	distribution network operator
DPSP	deficiency of power supply probability
DR	demand response
DSM	demand side management
ESS	energy storage system
LCC	life cycle cost
LCOE	levelized cost of electricity
LPSP	loss of power supply probability
MG	microgrid
MGO	microgrid operator
MMG	multiple microgrids
MOPSO	multi-objective particle swarm optimization
NMG	networked microgrids
P2P	peer-to-peer
PCC	point of common coupling
PSO	particle swarm optimization
PV	photo-voltaic
RE	renewable energy
REDR	renewable energy discard rate
REF	renewable energy factor
RES	renewable energy sources
T	total operating hours
TNPC	total net present cost
WT	wind turbine

Indices

b	index for buyer microgrids
d	index of day
i	index of microgrids
s	index for seller microgrids
t	index of hour
w	index of week

Parameters

η_c	charging efficiency
η_d	discharging efficiency
AEC_i	annual energy cost of MG_i
AEC_{NMG}	annual energy cost of NMG
$BE_i^{\max}$	maximum BESS energy allowable in MG_i
$BE_i^{\min}$	minimum BESS energy allowable in MG_i
BE_i^t	battery energy in MG_i at time t
$BP_{i,c}^{\min}$	minimum BESS charging power allowable in MG_i
$BP_{i,c}^{\max}$	maximum BESS charging power allowable in MG_i

$BP_{i,c}^{t}$	BESS charging power in MG_i at time t
$BP_{i,d}^{\max}$	maximum BESS discharging power allowable in MG_i
$BP_{i,d}^{\min}$	minimum BESS discharging power allowable in MG_i
$BP_{i,d}^{t}$	BESS discharging power in MG_i at time t
C_i^{EC}	energy purchase cost of MG_i from grid/NMG
$C_i^{EG,t}$	cost for energy purchased/sold by MG_i from grid during t
$C_i^{EMG,t}$	cost for energy purchased/sold by MG_i from NMG during t
C_i^{INV}	investment cost of MG_i
$C_i^{O\&M}$	operation & maintenance cost of MG_i
E_i^{IC}	investment cost of RES/BESS in MG_i
$E_i^{O\&M}$	operation & maintenance cost of RES/BESS in MG_i
E_i^{SI}	salvage cost of RES/BESS in MG_i
$E_{p,b}^{t}$	grid to peer energy trading price during t
$E_{p,s}^{t}$	peer to grid energy trading price during t
$E_{T,df}^{t}$	total deficit energy with buyer $MG's$ during t
$E_{T,ex}^{t}$	total excess energy with seller $MG's$ during t
I_i^{SL}	salvage income of MG_i
$I_i^{U,B}$	income of MG_i from utilization of BESS
$I_i^{U,RE}$	income of MG_i from utilization of RE
L_i	life time of RES/BESS in MG_i
$ld_{cy,i}$	load capacity in MG_i
$ld_i^{d,t}$	% load available in MG_i at time t during day d
ld_i^{t}	load in MG_i at time t
$ld_i^{w,t}$	% load available in MG_i at time t during week w
$LPSP_{MG_i}$	LPSP of individual MG_i
$LPSP_{NMG}$	LPSP of NMG framework
$MG_{i,sur}^{t}$	surplus energy in MG_i during t
$P_i^{G,cy}$	power generation capacity of each source in MG_i
$P_i^{G,RE,t}$	renewable energy generated in MG_i during t
$P_i^{U,RE,t}$	renewable energy utilized in MG_i during t
$PG_{s,b,i}^{t}$	energy bought/sold by MG_i during t from/to grid
$PMG_{b,i}^{t}$	energy bought by buyer MG_i during t
$PMG_{s,i}^{t}$	energy sold by seller MG_i during t
$PV_{al,i}^{t}$	% PV generation available in MG_i at time t
$PV_{cy,i}$	PV capacity in MG_i
PV_i^{t}	PV generation in MG_i at time t
$PV_{\min,i}$	minimum PV capacity in MG_i
$PV_{\max,i}$	maximum PV capacity in MG_i
$W_{al,i}^{t}$	% wind generation available in MG_i at time t
$W_{cy,i}$	wind capacity in MG_i
W_i^{t}	wind generation in MG_i at time t
$W_{\max,i}$	maximum wind capacity in MG_i
$W_{\min,i}$	minimum wind capacity in MG_i

Sets

B	set of buyers
N	total number of microgrids
S	set of sellers

DATA AVAILABILITY STATEMENT

Data sharing is not applicable to this article as no new data were created or analyzed in this study.

ORCID

Vankudoth Lokesh https://orcid.org/0000-0002-0906-118X

Altaf Q. H. Badar https://orcid.org/0000-0002-1572-3717

REFERENCES

1. IRENA (2022). *Renewable Power Generation Costs in 2021, Report*. Abu Dhabi: International Renewable Energy Agency; 2022.
2. Schmidt O, Melchior S, Hawkes A, Staffell I. Projecting the future levelized cost of electricity storage technologies. *Joule*. 2019;3(1):81-100.
3. E. I. A. (EIA). Battery Storage in the United States: An Update on Market Trends. https://www.eia.gov/analysis/studies/electricity/batterystorage/. 2021. Accessed January 13, 2023
4. Lasseter RH, Paigi P. Microgrid: a conceptual solution. *2004 IEEE 35th Annual Power Electronics Specialists Conference (IEEE Cat. No. 04CH37551)*. Vol 6. Aachen: IEEE; 2004:4285-4290.
5. Ton DT, Smith MA. The US department of energy's microgrid initiative. *Electr J*. 2012;25(8):84-94.
6. Farzin H, Moeini-Aghtaie M, Fotuhi-Firuzabad M. A hierarchical scheme for outage management in multi-microgrids. *Int Trans Electr Energy Syst*. 2016;26(9):2023-2037.
7. Yang H, Lu L, Zhou W. A novel optimization sizing model for hybrid solar-wind power generation system. *Solar Energy*. 2007;81(1):76-84.
8. Zhao G, Cao T, Wang Y, Zhou H, Zhang C, Wan C. Optimal sizing of isolated microgrid containing photovoltaic/photothermal/wind/diesel/battery. *Int J Photoenergy*. 2021;2021:1-19.
9. Mouachi R, Jallal MA, Gharnati F, Raoufi M. Multiobjective sizing of an autonomous hybrid microgrid using a multimodal delayed PSO algorithm: a case study of a fishing village. *Comput Intell Neurosci*. 2020;2020:1-18.
10. Fathy A, Kaaniche K, Alanazi TM. Recent approach based social spider optimizer for optimal sizing of hybrid pv/-wind/battery/diesel integrated microgrid in aljouf region. *IEEE Access*. 2020;8:57 630-57 645.
11. Haidar AM, Fakhar A, Helwig A. Sustainable energy planning for cost minimization of autonomous hybrid microgrid using combined multi-objective optimization algorithm. *Sustain Cities Soc*. 2020;62:102391.
12. De Clercq S, Zwaenepoel B, Vandevelde L. Optimal sizing of an industrial microgrid considering socio-organisational aspects. *IET Gener Transm Distrib*. 2018;12(14):3442-3451.
13. Muleta N, Badar AQ. Techno-economic analysis and design of hybrid renewable energy microgrid for rural electrification. *Energy Harvest Syst*. 2022;9(1):39-51.

14. Muleta N, Badar AQ. Designing of an optimal standalone hybrid renewable energy micro-grid model through different algorithms. *J Eng Res*. 2023;11(1):100011.
15. Che L, Zhang X, Shahidehpour M, Alabdulwahab A, Abusorrah A. Optimal interconnection planning of community microgrids with renewable energy sources. *IEEE Trans Smart Grid*. 2015;8(3):1054-1063.
16. Wang Y, Oulis-Rousis A, Strbac G. A three-level planning model for optimal sizing of networked microgrids considering a trade-off between resilience and cost. *IEEE Trans Power Syst*. 2021;36:5657-5669.
17. Xie H, Teng X, Xu Y, Wang Y. Optimal energy storage sizing for networked microgrids considering reliability and resilience. *IEEE Access*. 2019;7:86 336-86 348.
18. Mojtahedzadeh S, Ravadanegh SN, Haghifam M-R. Optimal multiple microgrids based forming of greenfield distribution network under uncertainty. *IET Renew Power Gener*. 2017;11(7):1059-1068.
19. Samadi Gazijahani F, Salehi J. Stochastic multi-objective framework for optimal dynamic planning of interconnected microgrids. *IET Renew Power Gener*. 2017;11(14):1749-1759.
20. Hakimi SM, Hasankhani A, Shafie-khah M, Catalão JP. Optimal sizing and siting of smart microgrid components under high renewables penetration considering demand response. *IET Renew Power Gener*. 2019;13(10):1809-1822.
21. Cao X, Wang J, Zeng B. Networked microgrids planning through chance constrained stochastic conic programming. *IEEE Trans Smart Grid*. 2019;10(6):6619-6628.
22. Wouters C, Fraga ES, James AM. An energy integrated, multi-microgrid, MILP (mixed-integer linear programming) approach for residential distributed energy system planning—a South Australian case-study. *Energy*. 2015;85:30-44.
23. Wang H, Huang J. Cooperative planning of renewable generations for interconnected microgrids. *IEEE Trans Smart Grid*. 2016;7(5):2486-2496.
24. Hakimi SM, Hasankhani A, Shafie-khah M, Catalão JP. Stochastic planning of a multi-microgrid considering integration of renewable energy resources and real-time electricity market. *Appl Energy*. 2021;298:117215.
25. Ghanbari A, Karimi H, Jadid S. Optimal planning and operation of multi-carrier networked microgrids considering multi-energy hubs in distribution networks. *Energy*. 2020;204:117936.
26. Ali L, Muyeen S, Bizhani H, Ghosh A. Optimal planning of clustered microgrid using a technique of cooperative game theory. *Electr Power Syst Res*. 2020;183:106262.
27. Ali L, Muyeen S, Bizhani H, Ghosh A. A peer-to-peer energy trading for a clustered microgrid—game theoretical approach. *Int J Electr Power Energy Syst*. 2021;133:107307.
28. Ali L, Muyeen S, Bizhani H, Ghosh A. A multi-objective optimization for planning of networked microgrid using a game theory for peer-to-peer energy trading scheme. *IET Gener Transm Distrib*. 2021;15:3423-3434.
29. Alam MN, Chakrabarti S, Liang X. A benchmark test system for networked microgrids. *IEEE Trans Ind Informatics*. 2020;16(10):6217-6230.
30. Kennedy J, Eberhart R. Particle swarm optimization. *Proceedings of ICNN'95-International Conference on Neural Networks*. Vol 4. Perth: IEEE; 1995:1942-1948.
31. Shi Y, Eberhart RC. Empirical study of particle swarm optimization. *Proceedings of the 1999 Congress on Evolutionary Computation-CEC99 (Cat. No. 99TH8406)*. Vol 3. Washington: IEEE; 1999:1945-1950.
32. Coello CC, Lechuga MS. MOPSO: a proposal for multiple objective particle swarm optimization. *Proceedings of the 2002 Congress on Evolutionary Computation. CEC'02 (Cat. No. 02TH8600)*. Vol 2. Honolulu: IEEE; 2002:1051-1056.
33. Coello CAC, Pulido GT, Lechuga MS. Handling multiple objectives with particle swarm optimization. *IEEE Trans Evol Comput*. 2004;8(3):256-279.

How to cite this article: Lokesh V, Badar AQH. Optimal sizing of RES and BESS in networked microgrids based on proportional peer-to-peer and peer-to-grid energy trading. *Energy Storage*. 2023; 5(7):e464. doi:10.1002/est2.464